Correlation of Stress and Atomic-Scale Surface Roughness Evolution during Intermittent Homoepitaxial Growth of (111)-Oriented Ag and Cu

C. Friesen and C.V. Thompson

Department of Materials and Engineering, Massachusetts Institute of Technology, Cambridge, Massachusetts 02139, USA

(Received 5 December 2003; published 30 July 2004)

Stress evolution during intermittent homoepitaxial growth of (111)-oriented Cu and Ag thin films has been studied. A tensile stress change is observed when growth is stopped, but the change is reversed when growth is resumed. Reflection high energy electron diffraction analysis of the atomic scale surface roughness during intermittent growth demonstrates a strong correlation between the surface structure and reversible stress evolution. The results are discussed in terms of an evolving surface defect population.

DOI: 10.1103/PhysRevLett.93.056104 PACS numbers: 68.55.Jk, 61.14.Hg, 68.37.–d

It has recently been shown that a tensile stress change occurs when Volmer-Weber growth of polycrystalline metallic thin films is interrupted and that this change is reversible in that resumption of growth leads to an evolution to the preinterruption stress magnitude and rate of change [1,2]. This reversible stress change is observed whether the preinterruption stress is tensile or compressive, and it increases with increasing preinterruption growth rate [2]. Further, there is a marked kinetic asymmetry between the stress evolution at the beginning of an interruption, and the much faster initial rate of stress recovery after resumption of growth. These reversible stress changes are observed at all stages of growth, from the nucleation and growth of isolated islands [3], through the coalescence stage [2], and into the continuous film regime [1,2]. It has been argued that reversible stress changes in the postcoalescence growth stage are associated with the development of excess surface steps [4] or reversible trapping of excess atoms at grain boundaries [5]. Alternatively, it has been suggested that these changes are associated with reversible changes in the concentration of adatoms [3] and other surface defects [2] that accumulate during all stages of Volmer-Weber growth.

It has been argued that the component of the stress change that is rapidly recovered when growth is resumed is associated with the generation of a nonequilibrium adatom concentration during growth. The undercoordinated adatoms interact with substrate atoms to generate a force dipole, resulting in a compressive stress in the surface [6]. In earlier work, a thermodynamic formalism was derived to relate the observed early-stage stress behavior to the force-dipole magnitude [2]. It was found that values extracted from experiments on continuous polycrystalline films compared well with embedded atom method molecular dynamics calculations of the force dipole.

When growth is first resumed after an interruption, the only change in the relaxed surface, and therefore the only source of stress, is the modification of the adatom population. However, as the growth process continues a number of different types of defects are created (e.g., surface vacancies, excess surface steps, etc.), and each of these defects leads to an associated modification of the average surface stress. Although it is straightforward to extract the contribution of the noninteracting adatoms to the stress evolution, it is more difficult to assign and sum the contributions of the entire set of defects that exist once a surface becomes rough on a multilayer scale. However, the ensemble of surface defects that result from the dynamic processes of growth leads to stresses that relax as the structures are eliminated through diffusive processes during growth interruptions.

Based on the arguments outlined above, reversible stress changes should be observed during interruptions of *homoepitaxial* growth for the same reasons they are observed during the growth of polycrystalline films. To test this expectation we have carried out experiments on homoepitaxial growth of epitaxial Ag and Cu films, materials used in earlier studies of polycrystalline films. While *in situ* stress measurements have been reported during epitaxial growth of metal films [7], there have not been reports of stress evolution during growth interruptions. We report observations of reversible stress changes during intermittent growth and also demonstrate a correlation with changes in surface defect concentrations, as indicated by *in situ* real-time reflection high-energy electron diffraction (RHEED).

The ultrahigh vacuum deposition system used in this study has a base pressure of 5×10^{-10} Torr and has three *e*-beam deposition sources and a quartz oscillator for use as a deposition rate monitor. This system is equipped with an all-electrical stress monitor that is introduced through the double-valued UHV loadlock chamber. Stress is monitored in real time as films are deposited on the cantilvever beam sample. Changes in stress at one surface of the cantilever cause the beam to bend, and the deflection is monitored by tracking the capacitance between a metal film on the backside of the beam and a fixed sensor. All of the components of the stress monitoring device, including the capacitance sensor and cantilever clamp, were machined into a single piece of glass ceramic. Because of the monolithic design of the device, sample placement error has been eliminated and the device is compact enough to fit through the chamber loadlock. This device can detect displacements of order 1 nm and has a bandwidth of 1 kHz. The UHV system is also equipped with a RHEED system. The RHEED system emits electrons at 10 keV and the configuration allows beam reflection at angles of incidence between 1° and 3°. The diffracted electrons illuminate a phosphor screen from which data are collected using a high resolution digital camera.

The RHEED technique samples the top few monolayers of a sample and therefore gives atomic scale information about the structure and morphology of surfaces. In the case of an atomically flat surface only the two-dimensional periodicity is represented in the Ewald sphere; therefore, in the absence of a diffraction condition in the out-of-plane direction, the diffraction pattern will consist of streaks. In the case of a surface that is rough on a length scale smaller than the mean free path of the 10 keV electrons (of order 100 Å [8]), a Bragg condition associated with the three-dimensional periodicity of the lattice results in diffraction spots. Therefore, by tracking the relative "streakiness" of the diffraction pattern, it is possible to qualitatively track the atomic scale surface roughness, within the above mentioned limits [9]. RHEED has been widely used to demonstrate the relaxation of surface roughness after interruptions of growth of epitaxial compound semiconductors, e.g., GaAs [10]. To our knowledge it has not been used to track surface roughness changes during the growth and growth interruptions of metal films when those films have been grown via electron-beam evaporation. The amount of light emitted by an *e*-beam deposition source filament is very high and is not constant, so that the magnitude and noisy nature of the light emitted by the deposition source makes collection and interpretation of the RHEED intensity pattern difficult to impossible. To eliminate this problem in the current experiment, a steel cone was constructed and inserted into the UHV system so that it was sealed to the phosphor screen and projected up to the sample. The cone was aligned such that electrons diffracted from the sample were collected through a 1 cm diameter orifice. The inside of the cone was also coated with graphite to reduce internal reflection. The addition of the cone also significantly reduced diffraction pattern expansion/contraction and shift effects due to changes in electric fields associated with the opening and the closing of the deposition shutter.

Samples were prepared by depositing 100 nm thick epitaxial Au films on 100 μm thick H-terminated Si(111) wafers and a subsequent backside Au film was deposited to act as a backplane for the capacitance measurement. The films were analyzed through both transmission electron diffraction and x-ray pole figure characterization. The relative spread in the in-plane and out-of-plane orientations were ±2.9° and 0.17°, respectively.

Transmission electron microscopy (TEM) indicated a relatively high dislocation density, but no clearly defined domain or low-angle grain boundaries. The samples were cut into the 1 cm × 3 cm cantilever geometry for the stress measurements or into the 1 cm square RHEED sample geometry. Once the samples were loaded either into the stress monitor or on the RHEED sample jig they were introduced through the loadlock into the system. A 100 nm thick continuous Cu or Ag film was then grown on the sample and the epitaxial character was confirmed through *in situ* RHEED analysis and through postexperiment *ex situ* x-ray diffraction and TEM analysis. The Cu films were fully relaxed and the Ag films did not detectably relax due to their near-perfect lattice match with the Au. After the films were grown, 24 h were allowed before further RHEED or stress experiments were performed. During the experiments the deposition rate was held at a constant 1 A/s and the samples were shuttered during the growth interruption phases of the experiments. All experiments shown here were performed at a nominal substrate temperature of 300 K. Figure 1 shows a topographic image of the intensity of one of the RHEED patterns captured during the Cu experiments. All of the RHEED patterns described herein were taken along the ⟨110⟩ azimuth. The highlighted ⟨1 0⟩-type diffraction spot on the lower left was used to track the spot length throughout the experiment.

The Cu experiments consisted of two growth phases lasting 50 s each (corresponding to growth of 50 A), and two growth interruptions of 50 s duration each. Figure 2 shows the results for both the stress measurements and RHEED spot length data. Note the similarities between

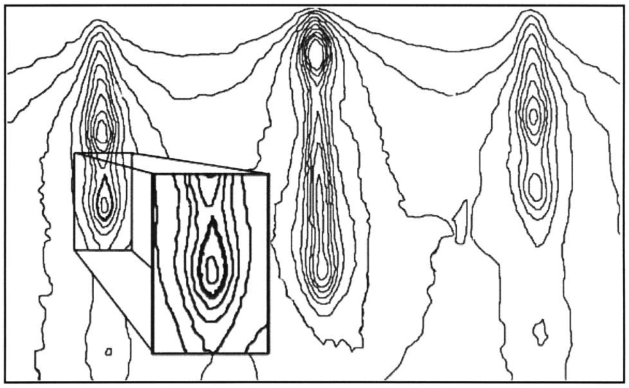

FIG. 1. Topographic representation of the RHEED pattern intensity observed during the growth of Cu/Cu(111). The thickened isointensity line within the highlighted region represents the value used to track the surface roughness.

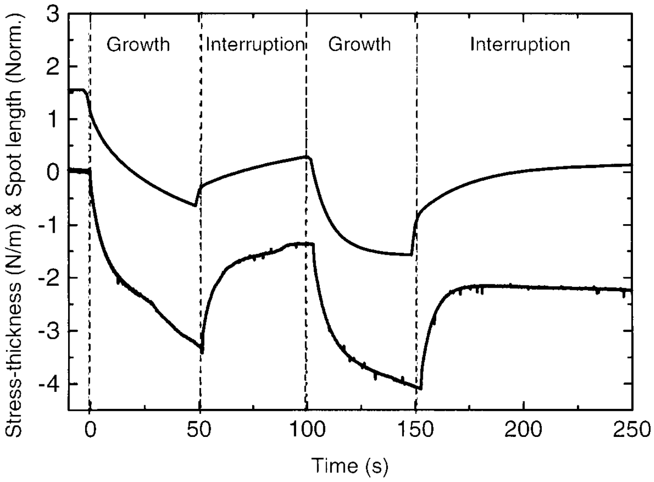

FIG. 2. The Cu/Cu(111) system stress thickness (bottom) and RHEED spot length (top) as a function of time.

the reversible stress evolution and the surface roughness. The reversible nature of the stress data is mirrored in the RHEED data. Also note that the initial slope of the stress curve at the beginning of growth is much larger (a vertical line on the time scale shown) than that of the RHEED data.

The Ag experiments consisted of a single 100 s growth period followed by a growth interruption of indefinite length, leading to the results shown in Fig. 3. Again, as in the Cu system, there is a correlation in the stress change and a surface structure change when growth is interrupted. Also, although the average stress is evolving toward a tensile state during growth, the stress change during the growth interruption is still in the tensile direction, demonstrating that reversible stress change does not result from a relaxation of the film stress.

Both Cu and Ag (111)-oriented homoepitaxial films grow in the "three-dimensional" or "multilayer" growth mode at room temperature [11,12]. This kinetic roughening is due to a low interlayer adatom diffusion that results from the relatively large Ehrlich-Schwoebel barrier for close-packed surfaces of fcc metals [11,13]. Thus, the adsorbed flux tends to either be incorporated at the upstep of the adsorbing terrace or form critical nuclei of two or more atoms, becoming essentially immobile. Flux impinging on these islands then leads to the nucleation of new islands, and growth proceeds through a "wedding cake–type" mode. The low interlayer mobility of the adatoms and the high probability of nucleation results in a rapid accumulation of defects ranging from adatoms and adatom vacancies to a large density of step ledges. Small multilayer islands on the order of tens of angstroms in diameter can lead to large step densities, which can greatly modify the measured average surface stress. When growth is interrupted, this roughness decays, but it is kinetically limited by the large Ehrlich-Schwoebel barrier.

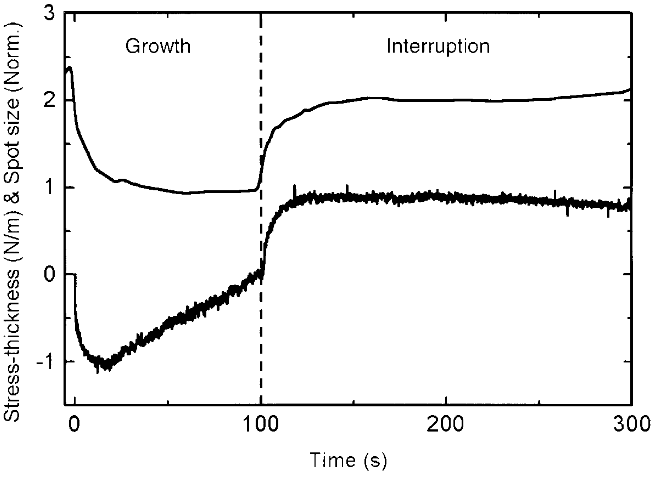

FIG. 3. The Ag/Ag(111) system stress thickness (bottom) and RHEED spot length (top) evolution as a function of time.

Each type of defect adds both a modification to the surface stress and a different time scale to the stress evolution. The compressive stress resulting from the addition of adatoms does not require diffusion, while the reduction of the excess adatom concentration does require diffusion. The creation of small multilayered islands also requires little diffusion during growth, while down-step diffusion and the relaxation of the islands takes much longer. The buildup and decay of these surface defects leads to the observed reversible stress and structure changes, with the observed kinetic asymmetry resulting from the different mechanisms required for the accumulation and reduction of the excess surface defects.

The instantaneous stress (partial derivative of the stress thickness with respect to thickness) in the Cu system just after the shutter was opened had an average value of 9.663 ± 1.307 GPa. Utilizing the thermodynamic formalism derived in [2], the instantaneous stress above corresponds to an adatom-surface force dipole of magnitude 0.710 ± 0.096 eV, which compares well with the previously reported value of 0.67 ± 0.079 eV for (111)-textured polycrystalline Cu films. Using nine total growth phases (data not shown) the average instantaneous stress in the Ag homoepitaxy system was 3.669 ± 0.94 GPa, which corresponds to an adatom surface interaction of 0.441 ± 0.113 eV. Embedded atom method calculations of the force-dipole magnitude for these systems result in a value of 0.572 eV for Cu and 0.430 eV for Ag. On the time scale of Figs. 2 and 3, the initial stress evolution appears to have an infinite slope; however, the RHEED data do not evolve as rapidly. In the first moments of the growth interruptions, the slope of the stress thickness versus thickness curve is large and positive, a vertical line on the time scale shown. Again, the diffraction results evolve more slowly. On a longer time scale the stress evolution also appears to reach a steady state faster than that of the RHEED results. These results are consistent with the expectation that isolated atomic defects such as adatoms do not significantly affect the RHEED pattern. They also indicate that some of the defects that result in RHEED spot changes do not significantly affect the stress.

The change in the surface stress is given by $\Delta f = -\beta\eta a\rho^{\text{step}} - \gamma\eta a\rho^{\text{kink}} - A\rho^{\text{adatom}} + \cdots$, where β, η, and a are the magnitude of the step-face surface stress (energy/step atom), the step height, and the inverse of the step-face area per atom [14], respectively, and ρ^{step} is the step density (#/length), γ is the kinked step-face surface stress, ρ^{kink} is the kink density (#/length), A is the adatom force-dipole magnitude, and ρ^{adatom} is the adatom density. The approximate value of A is 0.572 eV/atom [2]. A simple bond order argument gives the same formation energy for a kink as a step, so that the addition of kinks serves only as an effective increase in step length. β and γ are therefore estimated to be 0.59 eV/atom from bond-order arguments for the formation of a step on the Cu(111), based on a cohesive energy of 3.544 eV [15].

It is difficult to suggest a reasonable density for the transient defects present during growth, since all experimental evidence that exists is either from data collected during growth interruptions or is qualitative (as in the case of our experiments). However, it has been found that at steady state and 300 K, STM images of Cu(111) and Ag(111) steps are not well defined [16] because the density of defects near step ledges (adatoms emitted by the steps, kinks, etc.) is large. If we estimate that the average atomic-scale defect has an elastic component of interaction equal to 0.5 eV (as argued above), not taking into account defect-defect interaction, more than 50% of the surface during growth must be covered by these average defects to get a reversible stress equal to that observed in the Cu system. From this we conclude that defect-defect interactions significantly contribute to the observed surface stress. In the case of adatoms, the contribution of defect-defect interactions at 1/3 coverage can double the surface stress calculated when interactions are not considered, and this effect continues to grow with higher coverages [17]. Similar effects are expected for other defects such as steps and kinks. A complete accounting of all of the defects present during growth and all of the interactions among them could significantly reduce the defect density required to explain our experimental observations.

In summary, reversible stress changes have been observed during interruptions of homoepitaxial growth of (111)-oriented Cu and Ag epitaxial films. These changes are similar in both magnitude and kinetics to those observed during growth of polycrystalline films of the same materials. For growth of homoepitaxial and continuous polycrystalline films, analysis of the initial instantaneous stress after the resumption of growth indicates a dominant role for an increased adatom population. Reversible changes in RHEED patterns have also been observed to correlate with latter-stage stress evolution before and after interruptions of homoepitaxial growth. These changes occur at a stage in which multilayer surface roughening or smoothing is expected to significantly contribute to the surface stress. This result supports the suggestion that reversible stress changes during interruptions of film growth are associated with changes in the atomic scale surface structure. *In situ* highly sensitive stress measurements provide a quantitative real-time measure of surface evolution during film growth and during postgrowth smoothing of surfaces.

This work was supported by the National Science Foundation through Contract No. DMR-0302044. The authors thank Karl Sieradzki and Frans Spaepen for useful discussions.

[1] A. Shull and F. Spaepen, J. Appl. Phys. **80**, 6243 (1996).
[2] C. Friesen, S. C. Seel, and C. V. Thompson, J. Appl. Phys. **95**, 1011 (2004).
[3] C. Friesen and C. V. Thompson, Phys. Rev. Lett. **89**, 126103 (2002).
[4] F. Spaepen, Acta Mater. **48**, 31 (2000).
[5] E. Chason, B. W. Sheldon, L. B. Freund, J. A. Floro, and S. J. Hearne, Phys. Rev. Lett. **88**, 156103 (2002).
[6] K. H. Lau and W. Kohn, Surf. Sci. **65**, 607 (1977).
[7] D. Sander, S. Ouazi, V. S. Stepanyuk, D. I. Bazhanov, and J. Kirschner, Surf. Sci. **512**, 281 (2002).
[8] D. R. Penn, Phys. Rev. B **35**, 482 (1987).
[9] O. P. Karpenko, S. M. Yalisove, and D. J. Eaglesham, J. Appl. Phys. **82**, 1157 (1997).
[10] J. H. Neave, B. A. Joyce, P. J. Dobson, and N. Norton, Appl. Phys. A **31**, 1 (1983).
[11] M. Henzler, Surf. Sci. **357**, 809 (1996).
[12] H. A. van der Vegt, H. M van Pinxteren, M. Lohmeier, and E. Vlieg, Phys. Rev. Lett. **68**, 3335 (1992).
[13] J. Vrijmoeth, H. A. van der Vegt, J. A. Meyer, E. Vlieg, and R. J. Behm, Phys. Rev. Lett. **72**, 3843 (1994).
[14] V. I. Marchenko and A. Y. Parshin, Sov. Phys. JETP **52**, 129 (1981).
[15] C. Kittel, *Introduction to Solid State Physics* (Wiley, New York, 1966).
[16] M. Geisen, Prog. Surf. Sci. **68**, 1 (2001).
[17] R. V. Kukta, D. Kouris, and K. Sieradzki, J. Mech. Phys. Solids **51**, 1243 (2003).